Organic & Biomolecular Chemistry

ROYAL SOCIETY OF CHEMISTRY

COMMUNICATION

View Article Online
View Journal | View Issue

Cite this: *Org. Biomol. Chem.*, 2025, **23**, 4641

Received 9th February 2025,
Accepted 3rd April 2025

DOI: 10.1039/d5ob00228a

rsc.li/obc

Display selection of peptide ligands for helical aromatic foldamers†

Lingfei Wang,[a] Joseph M. Rogers, ‡[b] Simon J. Dawson,[c] Line M. Langhorn,[a] Ryan T. Howard,[a] Sunbum Kwon, §[a] Céline Douat, *[a] Hiroaki Suga *[b] and Ivan Huc *[a,c]

Helical aromatic oligoamide foldamers with a cluster of five biogenic side chains at their surface were designed and synthesized. Display selection of thioether macrocyclic peptides against these targets generated low micromolar binders that are highly selective for the side-chain arrangement.

Aromatic oligoamides – oligoamides having aryl groups in their main chain – are privileged scaffolds that interact with biopolymers.[1] This large class of compounds includes natural products,[2] old drugs like suramin that can bind to a range of proteins,[3] and rod-like[4] and helically folded[5,6] synthetic oligomers equipped with biogenic side chains. Our own efforts have been focused on the latter grouping that includes sizeable (1–15 kDa) and structurally well-defined molecules potentially able to bind to proteins through large contact surface areas.[5c] Methods to identify helical aromatic oligoamides that interact with a given protein target have included screening of small libraries[5c–e] and mimicry of α-helix side chain presentation[5b] or of B-DNA shape and negative charge distribution.[6] Aromatic amino acids¶ may also be combined with α-amino acids in hybrid sequences,[7] some of which are compatible with *in vitro* ribosomal peptide expression[8] and amenable to display selection against protein targets.[9] To further explore the scope of aromatic oligoamide recognition of proteins or peptides, it is relevant not only to screen or design synthetic aromatic oligoamides with affinity for a given target, but also to screen potential binders to a given aromatic oligoamide target. If a large library of proteins can be used to find a specific foldamer binder, then a large library of foldamers may as well be used to find a specific protein binder. For example, we recently reported that pull-down experiments allowed for the identification of nanomolar protein binders to a given helical aromatic foldamer out of the pool of proteins contained in a cell lysate.[10] Similarly, phage display selection allowed for the identification of affimers – protein binders – for α-helix mimicking foldamers.[11] However, it is not yet known if these aromatic oligoamides are capable of interacting with short peptides.

Here, we report on the successful display selection of thioether-macrocyclic peptides (teMPs) using the random non-standard peptides integrated discovery (RaPID)[12] system for the selective recognition of aromatic foldamer helices having a deliberately reduced target area. Reducing the binding area on the target molecule created a challenge for peptide macrocycle display selection. Indeed, unlike for nucleic acid aptamers[13] and in contrast to the success of the display selection of peptides against protein targets[12,14] or other large substrates like polymers and solids,[15] examples of successful display selections of peptides against small molecules are rare.[16] Our results thus highlight both the potential of aromatic helical foldamers to recognize peptides and the potential of cyclic peptides to recognize a smaller target.

The folding of oligoamides of 8-amino-2-quinoline carboxylic acid Q^X (Fig. 1b) into stable aromatic helices has been thoroughly described.[17] Their conformational stability is such that the equilibrium between the right-handed (*P*) and the left-handed (*M*) enantiomeric helical conformers of an octamer is kinetically inert in water at 25 °C.[18] Methods to introduce a variety of biogenic side chains on Q^X monomers without impacting helix stability are also available.[5b,19] We synthesized an aromatic oligoamide target potentially suitable for interaction with a peptide ligand: dodecameric sequence **1a** which contains five monomers carrying biogenic side chains (hydro-

[a]*Department Pharmazie, Ludwig-Maximilians-Universität München, Butenandtstr. 5-13, 81377 München, Germany. E-mail: celine.douat@cup.lmu.de, ivan.huc@cup.lmu.de*

[b]*Department of Chemistry, School of Science, The University of Tokyo, 7-3-1 Hongo, Bunkyo, Tokyo113-0033, Japan. E-mail: hsuga@chem.s.u-tokyo.ac.jp*

[c]*CBMN (UMR5248), Univ. Bordeaux-CNRS-INP, Institut Européen de Chimie et Biologie, 2 rue Escarpit, 33600 Pessac, France*

†Electronic supplementary information (ESI) available: Supplementary figures, schemes and data, detailed experimental protocols and characterisation of new compounds. See DOI: https://doi.org/10.1039/d5ob00228a

‡Current address: Department of Drug Design and Pharmacology, University of Copenhagen, Copenhagen 2100, Denmark.

§Current address: Department of Chemistry, Chung-Ang University, 84 Heukseok-ro, Dongjak-gu, Seoul 06974, Republic of Korea.

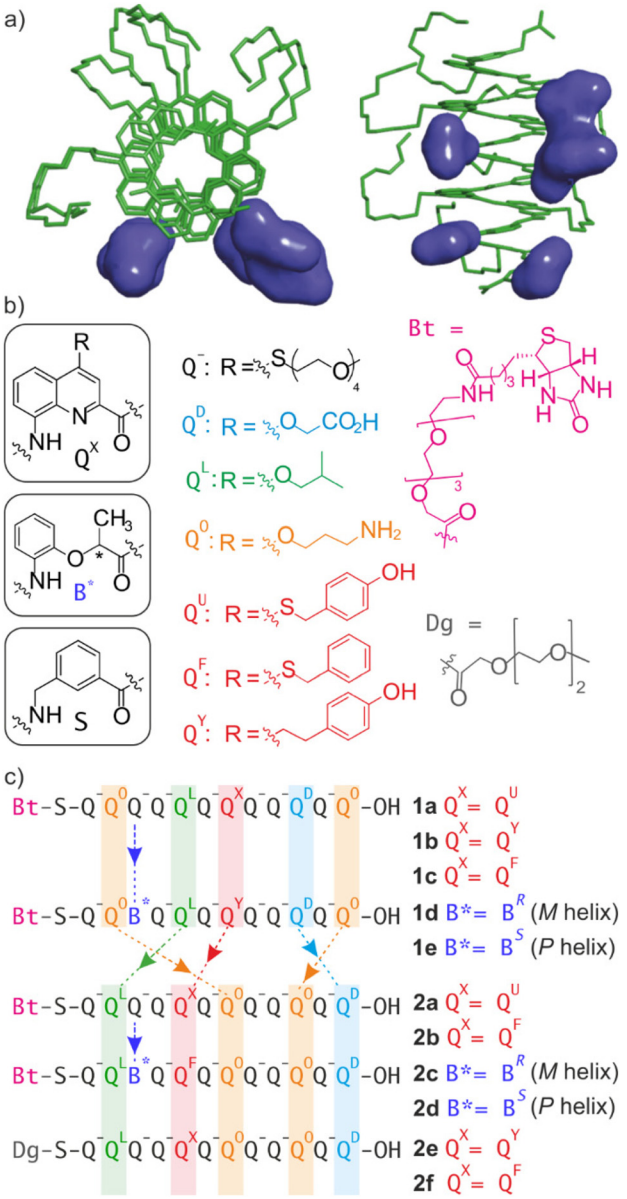

Fig. 1 (a) Top and side views of an energy-minimized model (MMFFs in Maestro)[22] of the aromatic helix of **1a**. The five clustered biogenic side chains are shown as solvent accessible surfaces. The main chain and tetraethylene glycol side chains are shown in green stick representation. (b) Formula of aromatic δ-amino acid residues (Q) colour coded according to their side chain: hydrophilic (black), hydrophobic (green), cationic (orange), blue (anionic), and red (aromatic). The chiral B* residue with *R* or *S* configuration, the spacer (S), and the chemical formula of the N-terminal functionalization of the foldamers (Bt or Dg) are also defined. (c) Synthesized foldamer sequences **1a–e** and **2a–f**. A one letter code has been used to define the side-chain or the chirality of the aromatic α-amino acids.

phobic leucine-like for Q^L, anionic aspartate-like for Q^D, cationic ornithine-like for Q^O, and aromatic tyrosine-like for Q^U), arranged in such a way that they form a cluster, *i.e.* a potential binding spot on one side of the helix (Fig. 1a and c). The seven other Q^- residues bear tetraethylene glycol side chains to provide water solubility and also to prevent peptide interactions outside of the binding spot.[20] We also synthesized sequence **2a**, an analogue of **1a** where the same biogenic residues are presented differently on the helix surface, to use as an alternative target and test the selectivity of peptide–foldamer interactions. Both sequences end with a 3-aminomethyl benzoic acid residue used as a spacer (S) separating the aromatic backbone from a biotin tail (Bt) intended for immobilization on streptavidin (SA). These foldamers are achiral and thus exist as a racemic mixture of *P*- and *M*-helical conformers. Both sequences were built on a solid support starting from a low-loading bromo-Wang resin and using *in situ* activation, as recently reported.[21] Crude purity was good and final purification was achieved using RP-HPLC (see the ESI† for details).

Sequences **1a** and **2a** were individually loaded on magnetic SA-beads and two independent RaPID selections were carried out in parallel to identify teMP binders. In the first selection, **1a** was the target with a counter-selection against the streptavidin on the solid support. In the second selection, **2a** was the target and **1a** on SA-beads was used for counter-selection. Thus, the second selection should in principle exclude teMPs that bind to areas present in both **1a** and **2a** like the helix cross-sections (the area decorated with Q^- is also shared by the sequences but it is not considered to be a plausible binding area). Since both the *P* and *M* helices are present, selections were simultaneously performed against two targets. The peptide precursor DNA library contained a coding region of ATG-(NNK)$_n$-TGC sequences, N is all 4 bases, K = T or G, and n = 8–15. This was transcribed to mRNA for *in vitro* translation, where the AUG start codon was reprogrammed with *N*-chloroacetylated-(L)-Trp (ClAc-W) for selection against **1a** and with chloroacetylated-(D)-Trp (ClAc-w)‖ for selection against **2a**. The repeats of NNK mixed codons encoded random α-amino acids and the TGC codon encoded a mandatory Cys to form a thioether macrocycle with the N-terminal chloroacetyl group. Of note, TGT was also present in the random NNK codons so additional Cys residues may appear earlier in the sequence. After the mandatory Cys, that is, nearer to the C-terminus, all peptides had a GSGSGS segment to act as a spacer between the cyclic peptide and the site where the encoding mRNA is attached.

Five iterative rounds of selection were performed before sequence analysis of the cDNA library (Fig. 2, S1 and S2†). The first selection led to strong convergence with twelve out of the top twenty ranked sequences showing more than 85% similarity, and the second to less extensive convergence. In both cases, the most amplified sequence (P1 and P2 in Fig. 2) contained two Cys residues. Based on previous studies,[7b,23] we considered that the smallest possible thioether macrocycle, that is, the macrocycle involving the Cys nearest to the N terminus, formed first during the spontaneous post-translational cyclization, giving rise to a lariat structure as found in other RaPID selections.[24] P1 thus consisted of an -Ac-WSTC- macrocycle with a linear peptide extension, and P2 of an -Ac-wSYGWC- macrocycle with a linear peptide extension. In both cases, the linear extensions contained several other hydro-

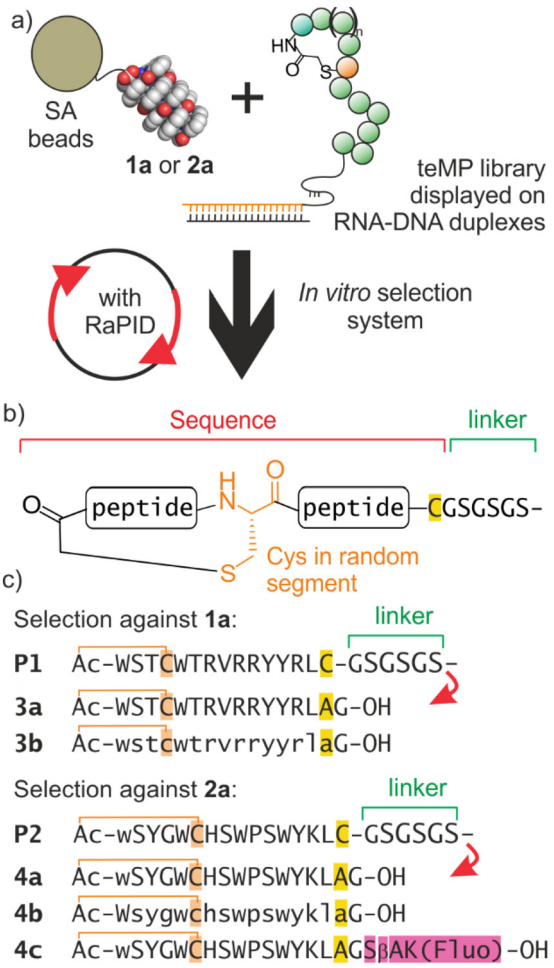

Fig. 2 (a) Overview of the *in vitro* selection of teMP binders for aromatic helical foldamers using the RaPID system. The biotinylated foldamers **1a** and **2a** were immobilized on SA-beads. (b) General structure of the selected teMPs. Peptide macrocyclization occurs *via* thioether formation from an N-terminal chloroacetyl group and a cysteine thiol which may be the mandatory Cys residue (highlighted in gold) or an earlier Cys in the random peptide segment. (c) Sequences of **P1** and **P2**, the most enriched peptides in the selections against **1a** and **2a**, respectively. These teMPs have a small macrocycle involving the first Cys in the sequence and a linear extension. Formulas of the synthesized lariat peptides **3a**, **3b**, **4a**, **4b**, and **4c**. Lowercase letters correspond to D amino acids. The orange line depicts the thioether linkage between the Cys thiol and N-terminal acetyl group. In these peptides, the C-terminal Cys was replaced with an alanine.

phobic residues (W, Y, P or L), suggesting that binding is driven by hydrophobic effects. For subsequent K_D determination, and to avoid possible issues with thiol oxidation, the C-terminal Cys was replaced with an Ala residue. Thus peptides **3a** and **4a** were prepared using standard solid phase peptide synthesis of a chloroacetylated precursor followed by resin cleavage and side-chain deprotection and by cyclization in a basic medium. The two teMPs were purified by semi-preparative RP-HPLC and characterized by LC-MS analysis.

At this stage, an unanticipated complication required our attention as we found that foldamers **1a** and **2a** slowly degraded. Upon standing in an aqueous medium, the *para*-hydroxybenzyl moiety of Q^u underwent 1,6-elimination to give 4-mercapto-quinoline. This degradation had been overlooked in sequences made previously that contained Q^U.[5d] We investigated side-chain instability using model pentamer **5** synthesized for that purpose (Fig. 3, S3 and S4†). The rate of elimination was found to vary with pH. It was slow enough for pH values between 5 and 7 to consider that elimination had been limited during the teMP RaPID selection. Nonetheless, the original target sequences **1a** and **2a** were judged unsuitable for physical investigations as degradation would reduce accuracy and reproducibility. We therefore prepared new foldamer sequences **1b–1e** and **2b–2f** in which Q^U was replaced either with Q^F, which bears a phenylalanine-like side chain similar to that of Q^U but lacking its hydroxy group, or with Q^Y which bears a tyrosine-like side chain with an ethylene connector instead of a thioether (Fig. 1b). Q^F and Q^Y do not differ from Q^U in the same way and it was not known whether these differences would matter so both were included in this study. The synthesis of Fmoc-$Q^{Y(tBu)}$-OH and Fmoc-Q^F-OH are reported in the ESI (Schemes S1 and S2†).

Peptide–foldamer interactions were first assessed using biolayer interferometry (BLI, Table 1, Fig. 4a, b and S5†). Biotinylated foldamers were independently loaded on SA-sensors and peptides were used as analytes in Tris buffer saline with Tween 20 (0.05%) and DMSO (0.1%) (TBST-D). The procedure is presented in detail in the ESI.† The observed kinetic curves showed a steady state regime, *i.e.* they reached a plateau value, and K_D values were determined using the Langmuir equation. Peptide **3a** from the first selection showed similar micromolar affinity for **1b** and **1c**, two analogues of the first selection target **1a**, suggesting that Q^F and Q^Y reproduce essential features of Q^U in this context. In contrast, in the

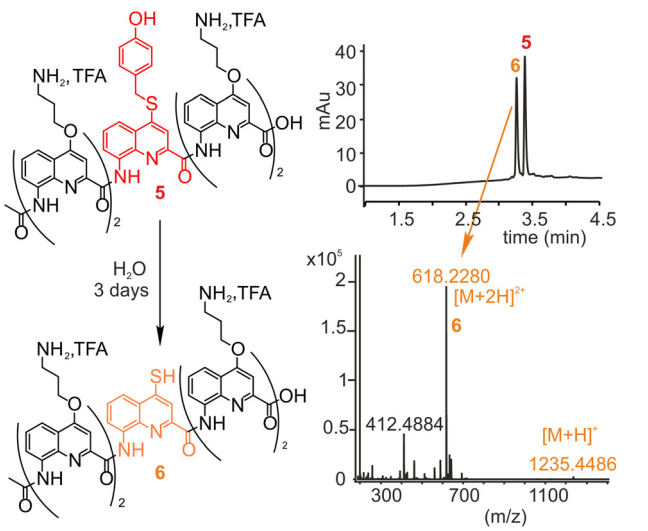

Fig. 3 Monitoring of the *para*-hydroxybenzyl side-chain elimination of Q^U in pure water on model pentamer **5**. The formation of the 4-mercapto-quinoline-containing pentamer **6** was confirmed by LC-MS analysis.

Table 1 K_D values (μM) determined by BLI

	Lariat peptide analyte			
Immobilized foldamer	**3a**	**3b**	**4a**	**4b**
1b	12.8 ± 0.3	—[b]	NBD[a]	—[b]
1c	19 ± 0.6	—[b]	—[b]	—[b]
1d (*M*)	9.5 ± 1.8	NBD	—[b]	—[b]
1e (*P*)	NBD[a]	10.3 ± 1.9	—[b]	—[b]
2b	NBD[a]	—[b]	16.1 ± 3.0	—[b]
2c (*M*)	—[b]	—[b]	NBD[a]	14.7 ± 2.2
2d (*P*)	—[b]	—[b]	9.7 ± 2.9	NBD[a]

[a] NBD indicates no binding detected. [b] A dash indicates that this measurement was not performed.

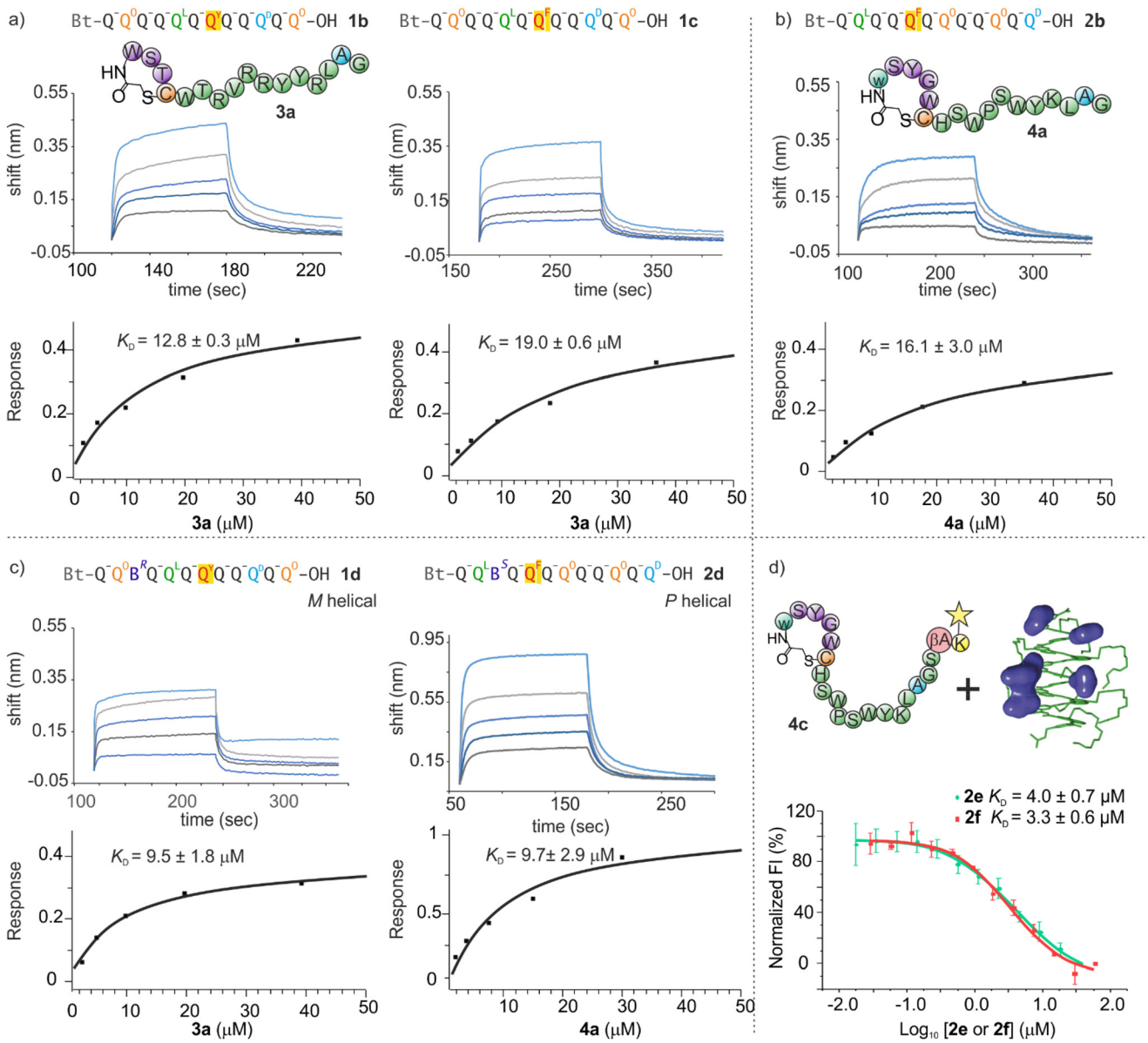

Fig. 4 BLI sensorgrams and steady state curve fittings to determine K_D values of the binding of (a) **3a** with **1b** and **1c** loaded on SA-sensor tips, (b) **4a** with **2b** loaded on SA-sensor tips, (c) **3a** with **1d** loaded on SA-sensor tips, and **4a** with **2d** loaded on SA-sensor tips. (d) Fluorescence intensity monitoring of the binding of fluorescein-labelled teMP **4c** and foldamers **2e** and **2f**. The binding assay results are from three independent experiments. Error bars represent the standard error of the mean of N = 3 experimental replicates.

same concentration range,** peptide **3a** showed no binding to **2b**, an analogue of the second selection target **2a**. This suggests that **3a** recognizes surface features unique to **1b** and **1c**, which excludes the aromatic helix cross-section also present in **2b**, and this is despite the absence of a counter-selection step against **2b** in the first selection. Similarly, peptide **4a** from the second selection showed micromolar affinity for **2b** and no binding to **1b** and **1c**. The observed selectivity thus points to the peptides targeting the small areas in which the biogenic side chains of their targets are clustered.

To consolidate these results, peptide–foldamer interactions were also assessed using a fluorescence assay as a second physical technique requiring no immobilization on a surface (Fig. 4d). Peptide **4c** was synthesized as an analogue of **4a** extended at its C-terminus using a Ser-β-Ala spacer and a fluorescein-labelled Lys. Concurrently, foldamers **2e** and **2f**, two analogues of **2a** having no biotin and either Q^F or Q^Y instead of Q^U, were prepared. Fluorescence was found to drop upon binding of the foldamers to the peptides. Peptide **4c** bound to **2e** and **2f** with K_D values of 4.0 μM and 3.4 μM, respectively. These values are slightly lower than those measured by BLI, and again show no significant differences between Q^F and Q^Y.

Next, we assessed the diastereoselectivity of the peptide foldamer interactions. The five Q^O (×2), Q^L, Q^D and $Q^{Y/F}$ biogenic side chains are not only projected differently in space at the surface of **1b** and **2b** but, for both compounds, the side chains are also projected differently in their *M* and *P* helical conformations, both of which were present during selection (Fig. S6†). We thus synthesized four new biotinylated foldamers, **1d**, **1e**, **2c** and **2d** (Fig. 1c). In each of them, the third residue (Q^-) was replaced with a chiral 2-(2-aminophenoxy)-propionic acid monomer (B* in Fig. 1b) with either (*R*) or (*S*) configuration. B^R and B^S have been shown to quantitatively bias the handedness of the aromatic helix to *M* (in **1d** and **2c**) and *P* (in **1e** and **2d**), respectively.[25] The extent of handedness bias was confirmed by ^{1}H NMR spectra where a single set of signals corresponding to only one (*R*–*M* or *S*–*P*) diastereomeric conformer is seen. The sign of helix handedness was controlled by circular dichroism spectroscopy. Each new foldamer was then individually immobilized on SA-sensor tips and their binding to peptides was assessed by BLI. These unveiled that the interactions are diastereoselective in the range of peptide concentrations used. teMP **3a** binds to *M*-helical **1d** and not to *P*-helical **1e**, while teMP **4a** binds to *P*-helical **2d** and not to *M*-helical **2c** (Table 1, Fig. 4c and S7†). It is noteworthy that the first selection has generated a binder selective for the *M* helix whereas the other selection yielded a binder selective for the *P* helix. The K_D values calculated from steady-state curve fitting are comparable to those obtained during the first round of BLI measurements on *P*/*M* helix mixtures, *i.e.* in the low micromolar range. Finally, we further validated the diastereoselective interactions in experiments where both the foldamer handedness and the peptide chirality were inverted. For that purpose, we prepared peptides **3b** and **4b**, the enantiomers of **3a** and **4a**, respectively. We found that the binding of **4b** to *M*-helical **2c** was similar to that of **4a** to *P*-helical **2d** (Table 1 and Fig. S8†). In the case of **3b**, measurements were first hampered by nonspecific binding of this D-peptide to the reference SA-sensor tips. This effect decreased sufficiently when adding 0.05% BSA to the TBST-D buffer and it could be again verified that the binding of **3b** to *P*-helical **1e** was similar to the binding of its enantiomer **3a** to *M*-helical **1d** (Table 1 and Fig. S8†).

Conclusions

In conclusion, despite the relatively small potential binding spot on the surface of the target helical aromatic oligoamide foldamers (only five biogenic side chains), the low molecular weight of the target (1.5 kDa, significantly smaller than typical RaPID protein targets),[12] and the highly non-proteinogenic chemistry, RaPID selections successfully delivered low micromolar binders that showed high selectivity for a specific arrangement of foldamer side chains. The specificity for the sequence of the foldamer biogenic side chains suggests that the cluster of biogenic side chains constitutes the teMP binding site. This specificity was further emphasized by the peptides' ability to selectively bind one handedness of the helical foldamer. Furthermore, the synthetic tractability of the peptides allowed for the synthesis of enantiomers to target the other handedness. Because of the moderate binding affinities in the low μM range, we did not invest further efforts in structural studies or systematic investigations of the sequence dependence of the interactions through, *e.g.*, Ala-scans. Nevertheless, our results highlight the high potential of aromatic foldamers equipped with biogenic side chains to interact with α-peptidic objects.

Author contributions

LW, JMR, SJD, LL, SK, and CD performed the experiments. CD, HS and IH supervised the research. All authors contributed to the writing, reviewing and editing of the manuscript and approved its final version.

Data availability

The data supporting this article have been included as part of the ESI.†

Conflicts of interest

There are no conflicts to declare.

Acknowledgements

This work was supported by the Deutsche Forschungsgemeinschaft (DFG) through project CRC1309-C7 (project ID 325871075) to I. H. and the JSPS Grant-in-Aid for

Specially Promoted Research (JP20H05618) to H. S. We thank Ivan Alonso for assistance with peptide synthesis and purification.

References

¶Aromatic groups bearing amine and carboxylic acid substituents. Amino acids with aryl groups in their side chains such as Phe, Tyr, Trp are also called "aromatic amino acids" but are not relevant here.

‖Changing the configuration of the N-terminal α-amino acid often results in the selection of different sequences (see ref. 12*d*). To explore new sequence space when targeting **2a**, we used "w" instead of "W".

**BLI experiments were typically performed up to teMP concentrations of 50 μM. At higher concentrations, teMP aggregation and nonspecific binding to SA-biosensors made it difficult to acquire reliable data.

1 T. Seedorf, A. Kirschning and D. Solga, *Chem. – Eur. J.*, 2021, **27**, 7321.

2 S. Baumann, J. Herrmann, R. Raju, H. Steinmetz, K. I. Mohr, S. Huttel, K. Harmrolfs, M. Stadler and R. Muller, *Angew. Chem., Int. Ed.*, 2014, **53**, 14605; E. Michalczyk, K. Hommernick, I. Behroz, M. Kulike, Z. Pakosz-Stepien, L. Mazurek, M. Seidel, M. Kunert, K. Santos, H. von Moeller, B. Loll, J. B. Weston, A. Mainz, J. G. Heddle, R. D. Sussmuth and D. Ghilarov, *Nat. Catal.*, 2023, **6**, 52; S. M. Hashimi, *J. Antibiot.*, 2019, **72**, 785; P. G. Baraldi, C. Nûnez, A. Espinosa and R. Romagnoli, *Curr. Top. Med. Chem.*, 2004, **4**, 231; Y. Hiraku, S. Oikawa and S. Kawanishi, *Nucleic Acids Symp. Ser.*, 2002, **2**, 95.

3 J. Zeelen, M. van Straaten, J. Verdi, A. Hempelmann, H. Hashemi, K. Perez, P. D. Jeffrey, S. Halg, N. Wiedemar, P. Maser, F. N. Papavasiliou and C. E. Stebbins, *Nat. Microbiol.*, 2021, **6**, 392; G. H. M. Salvador, T. R. Dreyer, A. A. S. Gomes, W. L. G. Cavalcante, J. I. Dos Santos, C. A. Gandin, M. de Oliveira Neto, M. Gallacci and M. R. M. Fontes, *Sci. Rep.*, 2018, **8**, 10317; L. Jiao, S. Ouyang, M. Liang, F. Niu, N. Shaw, W. Wu, W. Ding, C. Jin, Y. Peng, Y. Zhu, F. Zhang, T. Wang, C. Li, X. Zuo, C. H. Luan, D. Li and Z. J. Liu, *J. Virol.*, 2013, **87**, 6829; M. T. Murakami, E. Z. Arruda, P. A. Melo, A. B. Martinez, S. Calil-Elias, M. A. Tomaz, B. Lomonte, J. M. Gutierrez and R. K. Arni, *J. Mol. Biol.*, 2005, **350**, 416; G. H. M. Salvador, T. R. Dreyer, W. L. Cavalcante, F. F. Matioli, J. I. Dos Santos, A. Velazquez-Campoy, M. Gallacci and M. R. Fontes, *Acta Crystallogr.*, 2015, **71**, 2066; E. Mastrangelo, M. Pezzullo, D. Tarantino, R. Petazzi, F. Germani, D. Kramer, I. Robel, J. Rohayem, M. Bolognesi and M. Milani, *J. Mol. Biol.*, 2012, **419**, 198.

4 I. Saraogi, J. A. Hebda, J. Becerril, L. A. Estroff, A. D. Miranker and A. D. Hamilton, *Angew. Chem., Int. Ed.*, 2010, **49**, 736; T. Flack, C. Romain, A. J. P. White, P. R. Haycock and A. Barnard, *Org. Lett.*, 2019, **21**, 4433; R. A. Dohoney, J. A. Joseph, C. Baysah, A. G. Thomas, A. Siwakoti, T. D. Ball and S. Kumar, *ACS Chem. Biol.*, 2023, **18**, 1510; I. Arrata, C. M. Grison, H. M. Coubrough, P. Prabhakaran, M. A. Little, D. C. Tomlinson, M. E. Webb and A. J. Wilson, *Org. Biomol. Chem.*, 2019, **17**, 3861; G. M. Burslem, H. F. Kyle, A. L. Breeze, T. A. Edwards, A. Nelson, S. L. Warriner and A. J. Wilson, *ChemBioChem*, 2014, **15**, 1083; S. Kumar and A. D. Hamilton, *J. Am. Chem. Soc.*, 2017, **139**, 5744; J. P. Plante, T. Burnley, B. Malkova, M. E. Webb, S. L. Warriner, T. A. Edwards and A. J. Wilson, *Chem. Commun.*, 2009, **34**, 5091.

5 (*a*) J. M. Alex, V. Corvaglia, X. Hu, S. Engilberge, I. Huc and P. B. Crowley, *Chem. Commun.*, 2019, **55**, 11087; (*b*) M. Zwillinger, P. S. Reddy, B. Wicher, P. K. Mandal, M. Csékei, L. Fischer, A. Kotschy and I. Huc, *Chem. – Eur. J.*, 2020, **26**, 17366; (*c*) P. S. Reddy, B. Langlois d'Estaintot, T. Granier, C. D. Mackereth, L. Fischer and I. Huc, *Chem. – Eur. J.*, 2019, **25**, 11042; (*d*) J. Buratto, C. Colombo, M. Stupfel, S. J. Dawson, C. Dolain, B. Langlois d'Estaintot, L. Fischer, T. Granier, M. Laguerre, B. Gallois and I. Huc, *Angew. Chem., Int. Ed.*, 2014, **53**, 883; (*e*) S. Kumar, M. Birol, D. E. Schlamadinger, S. P. Wojcik, E. Rhoades and A. D. Miranker, *Nat. Commun.*, 2016, **7**, 11412; (*f*) J. Ahmed, T. C. Fitch, C. M. Donnelly, J. A. Joseph, T. D. Ball, M. M. Bassil, A. Son, C. Zhang, A. Ledreux, S. Horowitz, Y. Qin, D. Paredes and S. Kumar, *Nat. Commun.*, 2022, **13**, 2273.

6 V. Corvaglia, D. Carbajo, P. Prabhakaran, K. Ziach, P. K. Mandal, V. D. Santos, C. Legeay, R. Vogel, V. Parissi, P. Pourquier and I. Huc, *Nucleic Acids Res.*, 2019, **47**, 5511; V. Kleene, V. Corvaglia, E. Chacin, I. Forne, D. B. Konrad, P. Khosravani, C. Douat, C. F. Kurat, I. Huc and A. Imhof, *Nucleic Acids Res.*, 2023, **51**, 9629; D. Deepak, J. Wu, V. Corvaglia, L. Allmendinger, M. Scheckenbach, P. Tinnefeld and I. Huc, *Angew. Chem., Int. Ed.*, 2025, **64**, e202422958.

7 (*a*) M. Kudo, V. Maurizot, B. Kauffmann, A. Tanatani and I. Huc, *J. Am. Chem. Soc.*, 2013, **135**, 9628; (*b*) S. Dengler, C. Douat and I. Huc, *Angew. Chem., Int. Ed.*, 2022, **61**, e202211138.

8 C. Tsiamantas, S. Kwon, J. M. Rogers, C. Douat, I. Huc and H. Suga, *Angew. Chem., Int. Ed.*, 2020, **59**, 4860; C. Tsiamantas, S. Kwon, C. Douat, I. Huc and H. Suga, *Chem. Commun.*, 2019, **55**, 7366; J. M. Rogers, S. Kwon, S. J. Dawson, P. K. Mandal, H. Suga and I. Huc, *Nat. Chem.*, 2018, **10**, 405; O. Ad, K. S. Hoffman, A. G. Cairns, A. L. Featherston, S. J. Miller, D. Söll and A. Schepartz, *ACS Cent. Sci.*, 2019, **5**, 1289; T. Katoh and H. Suga, *J. Am. Chem. Soc.*, 2020, **142**, 16518.

9 T. Katoh and H. Suga, *J. Am. Chem. Soc.*, 2022, **144**, 2069; S. Dengler, R. T. Howard, V. Morozov, C. Tsiamantas, W.-E. Huang, Z. Liu, C. Dobrzanski, V. Pophristic, S. Brameyer, C. Douat, H. Suga and I. Huc, *Angew. Chem., Int. Ed.*, 2023, **62**, e202308408.

10 S. Kwon, V. Morozov, L. Wang, P. K. Mandal, S. Chaignepain, C. Douat and I. Huc, *Org. Biomol. Chem.*, 2024, **22**, 9342.

11 I. Arrata, A. Barnard, D. C. Tomlinson and A. J. Wilson, *Chem. Commun.*, 2017, **53**, 2834.

12 (*a*) Y. Goto and H. Suga, *Acc. Chem. Res.*, 2021, **54**, 3604; (*b*) Y. Yamagishi, I. Shoji, S. Miyagawa, T. Kawakami, T. Katoh, Y. Goto and H. Suga, *Chem. Biol.*, 2011, **18**, 1562;

(*c*) M. Nawatha, J. M. Rogers, S. M. Bonn, I. Livneh, B. Lemma, S. M. Mali, G. B. Vamisetti, H. Sun, B. Bercovich, Y. Huang, A. Ciechanover, D. Fushman, H. Suga and A. Brik, *Nat. Chem.*, 2019, **11**, 644; (*d*) T. Passioura, K. Watashi, K. Fukano, S. Shimura, W. Saso, R. Morishita, Y. Ogasawara, Y. Tanaka, M. Mizokami, C. Sureau, H. Suga and T. Wakita, *Cell Chem. Biol.*, 2018, **25**, 906.

13 A. Ruscito and M. C. DeRosa, *Front. Chem.*, 2016, 4; Y. Mu, Z. Chen, J. Zhan and J. Zhang, *Anal. Sens.*, 2024, **4**, e202400027.

14 S. You, G. McIntyre and T. Passioura, *Expert Opin. Drug Discovery*, 2024, **19**, 961.

15 T. Serizawa, T. Sawada, H. Matsuno, T. Matsubara and T. Sato, *J. Am. Chem. Soc.*, 2005, **127**, 13780; C. A. Stevens, F. Bachtiger, X.-D. Kong, L. A. Abriata, G. C. Sosso, M. I. Gibson and H.-A. Klok, *Nat. Commun.*, 2021, **12**, 2675; J. Bang, H. Park, J. Yoo, D. Lee, W. I. Choi, J. H. Lee, Y.-R. Lee, C. Kim, H. Koo and S. Kim, *Sci. Rep.*, 2020, **10**, 10576.

16 T. Sawada, Y. Okeya, M. Hashizume and T. Serizawa, *Chem. Commun.*, 2013, **49**, 5088.

17 H. Jiang, J. M. Leger and I. Huc, *J. Am. Chem. Soc.*, 2003, **125**, 3448; C. Dolain, A. Grelard, M. Laguerre, H. Jiang, V. Maurizot and I. Huc, *Chem. – Eur. J.*, 2005, **11**, 6135; T. Qi, V. Maurizot, H. Noguchi, T. Charoenraks, B. Kauffmann, M. Takafuji, H. Ihara and I. Huc, *Chem. Commun.*, 2012, **48**, 6337.

18 S. J. Dawson, Á. Mészáros, L. Pethő, C. Colombo, M. Csékei, A. Kotschy and I. Huc, *Eur. J. Org. Chem.*, 2014, 4265.

19 X. Hu, S. J. Dawson, P. K. Mandal, X. de Hatten, B. Baptiste and I. Huc, *Chem. Sci.*, 2017, **8**, 3741; M. Zwillinger, P. Sőregi, F. Sanchez, C. Douat, M. Csékei, I. Huc and A. Kotschy, *J. Org. Chem.*, 2025, **90**, 3043.

20 C. Bernhard, S. J. Roeters, J. Franz, T. Weidner, M. Bonn and G. Gonella, *Phys. Chem. Chem. Phys.*, 2017, **19**, 28182.

21 S. Dengler, P. K. Mandal, L. Allmendinger, C. Douat and I. Huc, *Chem. Sci.*, 2021, **12**, 11004; V. Corvaglia, F. Sanchez, F. S. Menke, C. Douat and I. Huc, *Chem. – Eur. J.*, 2023, **29**, e202300898.

22 *Maestro, Schrödinger*, LLC, New York, NY, 2021.

23 K. Iwasaki, Y. Goto, T. Katoh and H. Suga, *Org. Biomol. Chem.*, 2012, **10**, 5783.

24 H. Yu, P. Dranchak, Z. Li, R. MacArthur, M. S. Munson, N. Mehzabeen, N. J. Baird, K. P. Battalie, D. Ross, S. Lovell, C. K. Carlow, H. Suga and J. Inglese, *Nat. Commun.*, 2017, **8**, 14932.

25 D. Bindl, E. Heinemann, P. K. Mandal and I. Huc, *Chem. Commun.*, 2021, **57**, 5662.